Meteorol. Appl. 5, 253–261 (1998)

Different predictions by two NWP models of the surface pressure field east of Iceland

Haraldur Ólafsson, *Institute for Meteorological Research (RV) and Icelandic Meteorological Office (VÍ), Bustadavegi 9, IS-150 Reykjavik, Iceland*

In February and March 1996, the French NWP model Arpège was run to give operational forecasts five days ahead. These forecasts were a part of preparations for FASTEX (Fronts and Atlantic Storm-Track Experiment), whose field phase took place in 1997. The extensive collection and availability of model output during this period gave an excellent opportunity to study in real time the behaviour of different NWP models during the period of the year when strong winds and rapid changes in weather conditions are frequent. In this paper, we study a case where the ECMWF model predicted an incorrect pressure gradient at Northeast Iceland, while Arpège correctly simulated the gradient. The model errors are connected to anomalies in the mid-tropospheric vorticity field, which is in general quite different in the two models. The differences in the vorticity fields are discussed in relation to orographic effects.

1. Introduction

Significantly different forecasts from different numerical weather prediction (NWP) models is a well-known problem in operational weather forecasting. Generally, large differences in short-term forecasts originate in the initial fields, but elements such as different resolution or different parameterization schemes may also be responsible. Most often, the models' results converge as one gets closer in time to the point when the models are being compared. Thus, a 96-hour forecast by two operational models initialized at the same time may diverge greatly, while 48 hours later, the 48-hour forecast is less likely to give large differences.

Here, we present a study of a case where two models did not converge as the time comparison approached. At 0000 UTC on 24 February 1996, a 968 hPa cyclone was situated between Iceland and the British Isles. East of Iceland, there was a relatively deep trough in the surface pressure field, with a second minimum off the north-east cost of Iceland. The French model, Arpège, predicted consistently this trough, and a strong pressure gradient over Northeast Iceland, while the operational ECMWF model, equally consistent with itself, predicted only a flat and a more circular low, giving weak winds in Northeast Iceland.

An attempt will be made to analyse the processes that led to such different results. First, we shall give some basic information on the models, then we shall discuss the relevant dynamics. The geopotential tendency equation is presented and its terms are discussed in relation to orographic effects. We then compare the forecasts of pressure and vorticity fields by the two models. Finally, the vorticity production is discussed in relation to the characteristics of the NWP models.

2. The NWP models

Both the ECMWF model and Arpège are hydrostatic. The ECMWF model is run once every 24 hours, using initial fields that are based on the analysis at 1200 UTC. Arpège is run twice a day, at 0000 UTC and 1200 UTC. In less than three hours after the time of analysis, Arpège has prepared its initial fields and the model starts to integrate forwards in time. The cut-off time of the ECMWF model is considerably longer: up to about eight hours after the analysis time. The resolution of both models is given in terms of truncation, i.e. the number of waves the model may resolve at a given latitude.

The ECMWF model has a truncation of 213 (T213), which is constant in space. Arpège, on the other hand, has a space-dependent resolution, shown in Figure 1. The shaded area indicates where Arpège has better resolution than the ECMWF model. The maximum resolution of Arpège is centred over France, but the shaded area extends all the way to the east coast of Canada. Over southern Greenland, the truncation is about 300, and about 380 over Iceland. This is significantly greater than the resolution of the ECMWF model for the same areas. The better the resolution, the better we may expect the orography to be represented. A coarse grid tends to lower high mountains and represent topographic obstacles more poorly than fine-mesh models. Neither of the models has a so-called envelope orography (Lott & Miller, 1997; Geleyn *et al.*, 1994).

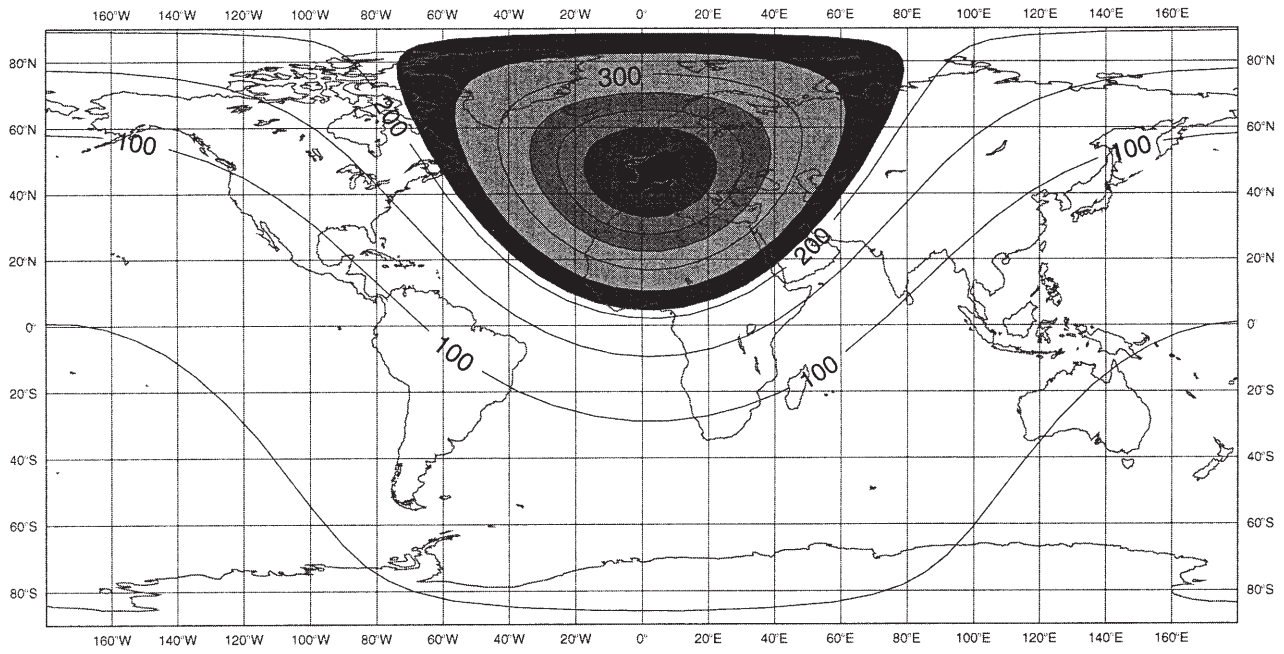

Figure 1. *The horizontal resolution (truncature) in Arpège. The shaded area is where Arpège has greater resolution than the ECMWF model (T213).*

3. The geopotential tendency, vorticity and orographic perturbations

For synoptic-scale hydrostatic flow on an f plane we have the geopotential tendency equation:

$$\left\{\nabla^2 + \frac{f^2}{\sigma}\frac{\partial^2}{\partial p^2}\right\}\frac{\partial \Phi}{\partial t} = -f\,\mathrm{V_g}\cdot\nabla\left\{\frac{1}{f}\nabla^2\Phi + f\right\} + \frac{f^2}{\sigma}\frac{\partial}{\partial p}\left\{-\mathrm{V_g}\cdot\nabla\frac{\partial \Phi}{\partial p}\right\} \quad (1)$$

where f is the Coriolis parameter, σ is a static stability parameter, p is the pressure, Φ is the geopotential and $\mathrm{V_g}$ is the geostrophic wind.

Through the hydrostatic equation, the pressure is proportional to the geopotential, provided the density is constant. The geostrophic vorticity is related to the geopotential by $\zeta_g = {}^1/_f \nabla^2\Phi$, and the quantity $\partial\Phi/\partial p$ is proportional to the temperature.

According to equation (1), contributions to pressure changes can come either from horizontal advection of absolute vorticity (first term on the right-hand side) or from differential advection of temperature. In general, the highest values of vorticity and strongest vorticity gradients are found in the middle or upper troposphere, while the temperature gradients are strongest in the lower troposphere. Thus, contributions to the first term on the right-hand side of equation (1) come mainly from the middle or upper troposphere, while the strong horizontal temperature gradients that often occur in the lower troposphere act through the second term.

Orographic obstacles in the atmospheric flow can modify both the vorticity and the temperature fields in many ways. Splitting of flow that meets an obstacle may force descent of warm air in the lee. Similarly, large-amplitude hydrostatic mountain waves bring down warm air, immediately downstream of the mountain top. This may result in strong temperature gradients between the wake and the surrounding flow. Mountains also generate vorticity and potential vorticity (PV) in stratified airflow. A major source of both is located on the shearline, where flow that has been accelerated and diverted to both sides of the mountain meets the slow flow in the wake. Schär & Smith (1993) and Schär & Durran (1997) have described generation of PV under such circumstances. Above the mountain top level, there is theoretically no shearline dividing the horizontally deflected flow and a wake. However, gravity waves generated by the mountain transport momentum vertically as far as the stratosphere, depending mainly on the vertical profile of wind and stability. The vertical transport of horizontal momentum is a fundamental property of hydrostatic mountain waves. It is related to the increased wind speed in the part of the wave where air is descending but decreased wind speed in the part of the wave where the air is rising (Figure 2).

Thus, above the edges of the mountain, where the flow with vertically propagating mountain waves meet the undisturbed flow, a horizontal wind shear is present and vorticity is thereby generated. If the wave is sufficiently steep (vertical isentropes in the 'SLOW FLOW' region in Figure 2), the air becomes convectively unstable and the wave breaks. Such mountain wave breaking resembles the breaking of ocean waves on a beach, except that the ocean waves break by falling forwards, while the mountain waves break by falling backwards.

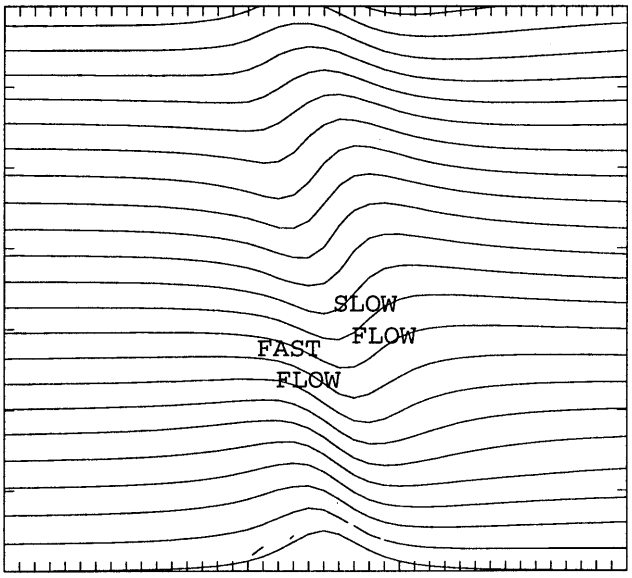

Figure 2. *Isentropes in a numerical simulation of a quasi-linear mountain wave. The flow is from left to right (from Ólafsson, 1996a).*

A breaking mountain wave returns the momentum to the main flow which decelerates and may even be reversed in the breaking zone. Consequently, the generation of vorticity by a horizontal wind shear between a breaking zone and undisturbed flow may be expected to be strong.

On a non-rotating plane, the occurrence of orographic flow splitting or large-amplitude or breaking waves is governed by the ratio Nh/U, where N is the Brunt–Väisälä frequency or the static stability of the air, h is the mountain height and U is the wind speed perpendicular to the mountain. Nh/U is often referred to as the inverse Froude number or the non-dimensional mountain height. Smith (1989) has developed a linear theory in density coordinates predicting the onset of flow splitting and wave breaking as a function of mountain aspect ratio (mountain width divided by mountain length) and Nh/U (Figure 3). According to this theory, the mountain waves break for values of Nh/U roughly between 1 and 2 for a mountain aspect ratio of 2 (which is close to the aspect ratio of Iceland in northerly flow). For Nh/U greater than about 1.2 (a value that increases with decreasing Rossby number), the low-level flow is split and deflected to both sides of the mountain. For a higher aspect ratio (e.g. Greenland in westerly flow), the limits of both flow splitting and wave breaking are moved to somewhat lower values of Nh/U. The presence of the Coriolis force can be expected to be of significance for flow past Greenland (low Rossby number), while for flow past Iceland, the rotation is of less importance (high Rossby number). In general, rotation reduces wave activity (Smith, 1979), but favours secondary wave breaking (breaking related to flow being accelerated and deflected round areas of high orography). Rotation also delays the onset of flow splitting (Ólafsson & Bougeault, 1997).

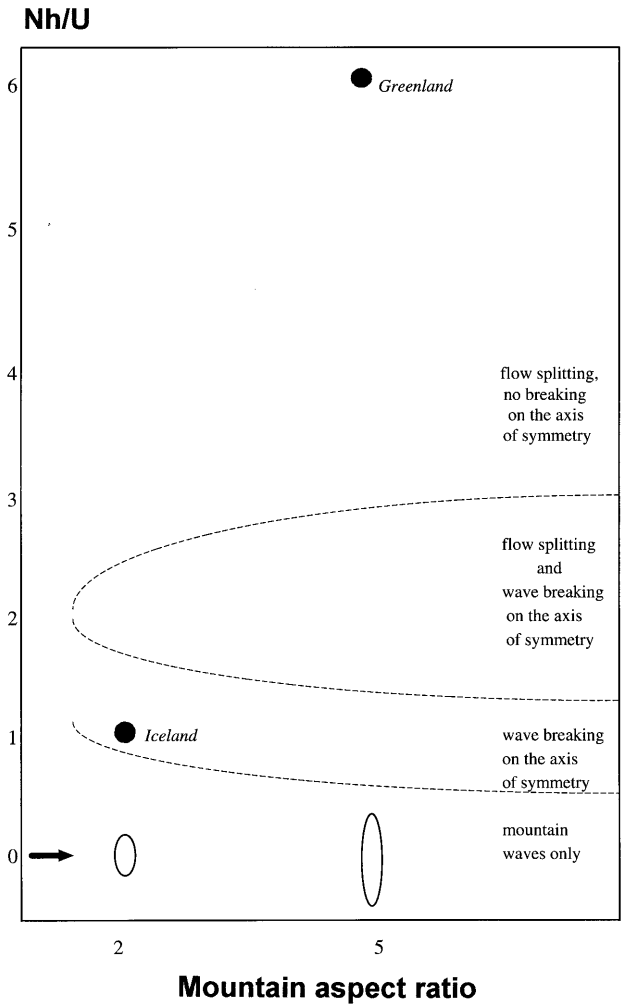

Figure 3. *Smith's (1989) flow regime diagram with modifications due to non-linear and rotational effects (Rossby number = 2.5), proposed by Ólafsson (1996b). The values of Nh/U for Iceland and Greenland are calculated by averaging U and N separately in a layer below mountain top level, upstream of the mountains.*

In our case, the values of Nh/U are close to 1 for Iceland and about 3 for Greenland, when N and U are averaged upstream in a layer between the surface and twice the height of the topography. In the context of flow splitting, it may be more appropriate to average between the surface and mountain top level. Calculating Nh/U in this way gives similar values for flow over Iceland, while the value of Nh/U for Greenland is more than doubled. Consequently, splitting and horizontal deflection must be an important feature of flow past Greenland, while wave breaing without flow splitting is expected over Iceland. Breaking over Iceland is also favoured by a wind decrease with altitude and a critical level (u = 0) at a mid-tropospheric level. The high value of Nh/U does not eliminate breaking of the Greenland mountain waves. In fact, owing to three-dimensional non-linear effects, breaking may be expected for Nh/U up to at least 6.8 (Ólafsson & Bougeault, 1996). For such high values of Nh/U, the zones of wave breaking and the associated windshear are expected to be located at the edges of the mountain ridge.

4. The different scenarios and evolution of the vorticity fields

The 36-hour forecasts of the sea-level pressure field on 24 February at 0000 UTC, together with the analysed surface pressure field, are shown in Figure 4. The ECMWF model places the low further west than Arpège, but our main interest is the difference in surface pressure north and north-east of Iceland. Here, Arpège gives an important trough that does not appear in the ECMWF output, which shows a more circular form of the low. The difference in the surface pressure gradient between the two models in this region corresponds to force 9 instead of force 4–5 on the Beaufort scale in north-eastern Iceland. Needless to say, such a difference in wind speed may distinguish between life and death for the crews of small fishing vessels. Concerning the shape of the trough and the pressure gradient, the Arpège scenario turned out to be much closer to reality, as presented in Figure 4(*c*), which shows an analysis of the sea surface pressure field, based only on observations, with no first-guess field involved.

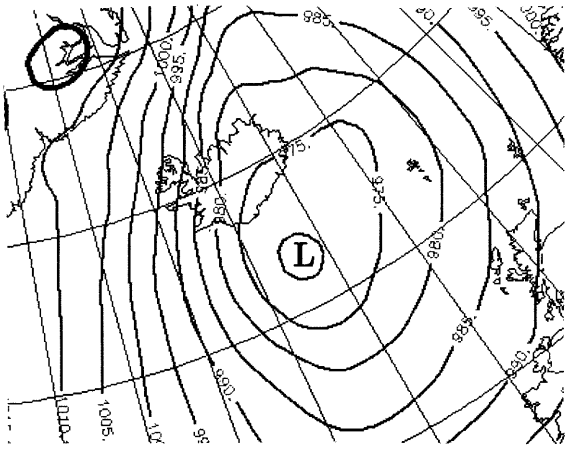

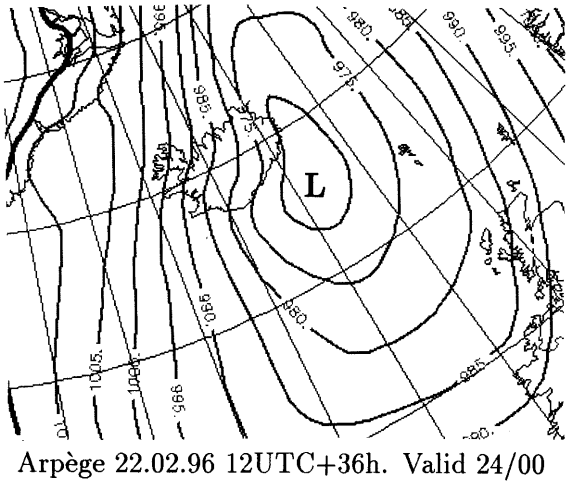

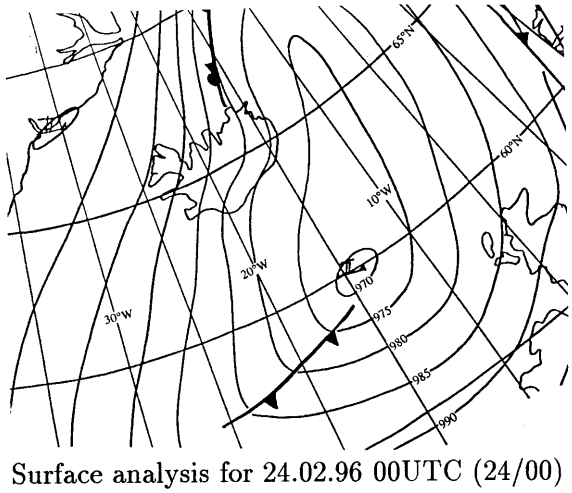

Figure 4. *Sea level pressure field as predicted by ECMWF and Arpège, and the surface analysis for 24 February 1996 at 0000 UTC*

Further comparison of the analysed field and the forecast of the two models shows that although the shape of the trough is more correct in the Arpège output, the value of simulated pressure is about 5 hPa too low everywhere along the north coast of Iceland as well as in the trough to the northeast of Iceland. In the ECMWF model, the pressure off the north-east coast of Iceland is almost correct, while the pressure at the north coast of Iceland turned out to be up to 9 hPa too low. At a previous stage the ECMWF model did indeed give a better-defined trough to the northeast of Iceland, but at 0000 UTC on 24 February this model had given a relative pressure rise in the trough. In the following, we shall attempt to analyse the processes in the models that led to such different results. First, we have to concentrate on the ECMWF model's underestimation of the surface pressure at the north coast of Iceland. Secondly, there will be a discussion on the origin of the relative pressure rise in the ECMWF trough.

According to equation (1), the difference in the pressure field may be related either to differential advection of temperature or to vorticity advection. Guided by equation (1), we shall attempt to trace the origin of the different model outputs. A study of the temperature fields (not shown) shows that advection of temperature is unable to explain the differences in forecast pressure in the two models. However, we find significant variations in the advection of cyclonic and even anticyclonic vorticity with a maximum at mid-tropospheric levels. Figure 5 shows the evolution of relative vorticity at 500 hPa in both models. At 24/0000 UTC, the ECMWF field shows a dipole structure to the north and the north-east of Iceland, while Arpège has no such structure. The anomaly of cyclonic (negative) vorticity at the north coast of Iceland appears to be responsible for the erroneously low surface pressure in this region, while a positive vorticity anomaly further to the east contributes to filling of the surface trough. The 500 hPa wind fields are not shown, but they may be roughly deduced from the vorticity field, since a maximum cyclonic vorticity is aligned with the jet. At the beginning of the sequence (22/1200 UTC), the jet blows from northwest to southeast over the southern part of

Greenland and ascends to the north over Iceland. At the end of the sequence (24/0000 UTC), the jet blows southward over the east coast of Greenland and to the north between Scotland and Iceland.

Strictly speaking, vorticity is not materially conserved, but experience shows that vorticity anomalies in the troposphere can be traced on weather maps for up to several dayss. In the following, we shall attempt to trace the origin of the vorticity anomalies in the ECMWF model.

(a) At 22/1800 UTC, the pressure at the east coast of Iceland is about the same as at the west coast, but the pressure in the east is falling and the northerly wind is about to start. The vorticity signatures in both the ECMWF model and Arpège at the south coast of Iceland are very much alike. As the northerly flow increases, the vorticity field in the lee of Iceland develops differently in the two models.
(b) At 23/0000 UTC, the ECMWF model shows a tripole pattern: two minima with a maximum in between. Arpège has a much smoother field with a vorticity maximum at the south-west coast of Iceland and an extended minimum far south of eastern Iceland.
(c) At 23/0600 UTC, the cyclonic (negative) vorticity south-east of Iceland has been advected to the north-east with a speed of 40–50 km h^{-1}. Our attention is now drawn to a dipole of negative and positive vorticity south of Iceland. No such dipole appears in the Arpège model.
(d) At 23/1200 UTC, the vorticity dipole is located to the southeast of Iceland.
(e) At 23/1800 UTC, the vorticity dipole has moved further north. The negative anomaly is now over the north-east coast of Iceland. More negative vorticity is created at the south coast of Ireland.
(f) At 24/0000 UTC, the time of comparison with the observed surface pressure field, the dipole structure in the ECMWF model has been advected further north, with the negative anomaly at the eastern part of the north coast of Iceland. As before, the positive anomaly is located further to the east, off the north-east coast of Iceland. The Arpège model has no such development, and at 24/0000 UTC, the vorticity field over Iceland is very smooth, with a positive vorticity anomaly close to the west coast and an extended negative vorticity anomaly to the east of Iceland. These anomalies are in fact also represented in the ECMWF model, but in addition to the smaller anomalies discussed above.

As stated above, the negative vorticity anomaly that we have now traced from the south coast to the north coast of Iceland appears to explain why the ECMWF model predicted far too low surface pressure at the north coast of Iceland. The associated positive vorticity anomaly corresponds on the other hand to the ECMWF model filling the trough that appears clearly in the Arpège output. By filling the trough, the ECMWF model did indeed bring the surface pressure in that area closer to reality, but this contributed to a wrong shape of the low and too weak winds in northeast Iceland. Therefore, we shall, in the following, focus on the origin of the positive vorticity anomaly that is located to the north-east of Iceland on 24/0000 UTC.

We have already traced the positive anomaly back to a location some 300 km south-east of Iceland six hours earlier. At 23/0600 UTC, there is a relatively large area with two peaks of little cyclonic vorticity south of Iceland. The one located further south corresponds to the anomaly six hours later if we suppose it travels with a constant speed of about 40 km h^{-1}. At 23/0000 UTC, the anomaly is located to the south-south-west of Iceland and is relatively weak. At 22/1800 UTC, our vorticity minimum has moved further west along about 59° N and is located at 30° W. Again, it appears only as a ridge between anomalies of strong vorticity. Continuing further backwards in time brings us to the analysis on 22/1200 UTC, where the anomaly is located at 60° N and 35° W. Here, the ECMWF model shows in general a clear signature of oscillations in the vorticity field, giving local minima and maxima, while Arpège has only a smooth and extended minimum in the lee of Greenland. Upstream of Greenland, the models are quite alike and we conclude that differences in the vorticity fields in the two models are related to different representation of the impact that the Greenland and Iceland relief has on the flow. In other words, it appears that some orographic effects, introduced in the ECMWF model in the lee of Iceland and Greenland contributed to its poor forecast in the north-east of Iceland.

5. Discussion

In the previous section, we related differences in the sea level pressure field, forecast by two numerical models, to different structures of the mid-tropospheric vorticity fields. Unlike the French Arpège model, the ECMWF model has a vorticity field characterized by frequent maxima and minima. The forecasting error in the ECMWF model is related to these peaks, which apparently are being advected along the northern side of the jet from their origin, in the lee of Iceland and Greenland.

Why are the vorticity fields so different in the two models? In view of the fact that Arpège has a better resolution over Greenland and Iceland, one would expect it to give a more detailed or less smooth vorticity field than the coarse-gridded ECMWF model. However, Figure 5 reveals the contrary: Arpège ‘misses’ the mesoscale signatures, including the vorticity anomalies that gave too low surface pressure at the north coast of Iceland and filled the trough in the ECMWF model.

ECMWF analysis for 22.02.96 12UTC

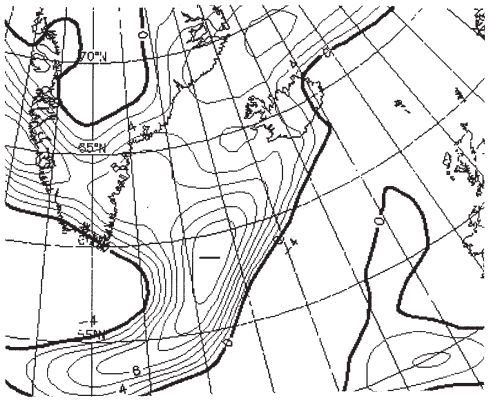

Arpège analysis for 22.02.96 12UTC

ECMWF 22.02.96 12UTC+6h. Valid 22/18

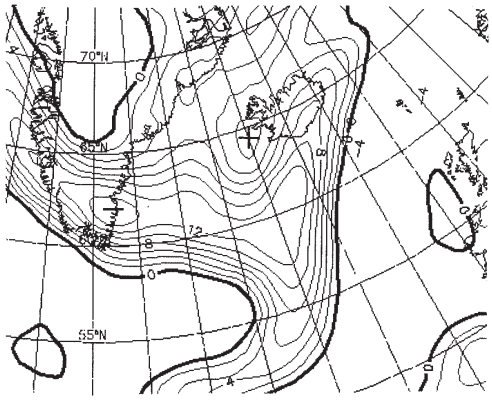

Arpège 22.02.96 12UTC+6h. Valid 22/18

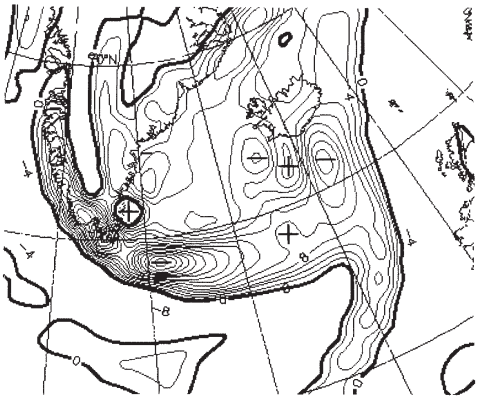

ECMWF 22.02.96 12UTC+12h. Valid 23/00

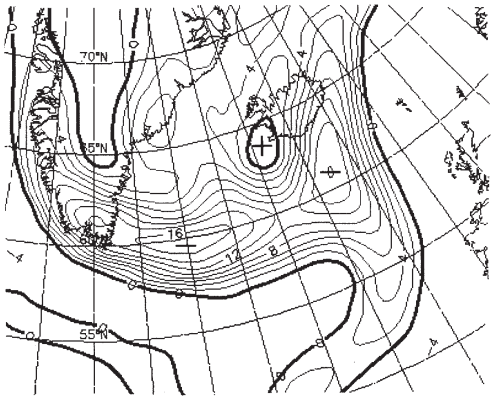

Arpège 22.02.96 12UTC+12h. Valid 23/00

Figure 5. *Relative vorticity at 500 hPa in the ECMWF and Arpège outputs. The zero vorticity isoline is bold; anomalies of much cyclonic vorticity are indicated by a minus (–) and anomalies of little cyclonic vorticity or anticyclonic vorticity are indicated by a plus (+). Isolines are for every* 2×10^{-5} s^{-1}.

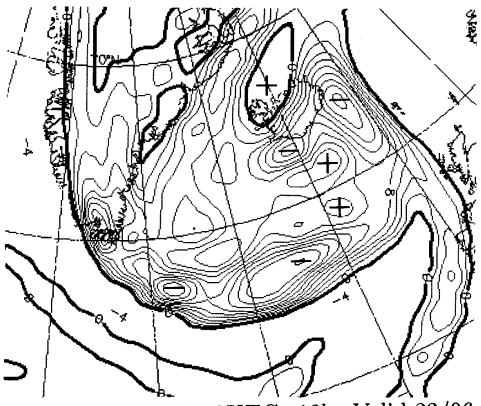

ECMWF 22.02.96 12UTC+18h. Valid 23/06

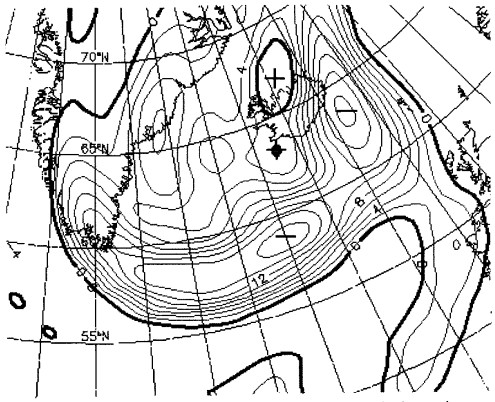

Arpège 22.02.96 12UTC+18h. Valid 23/06

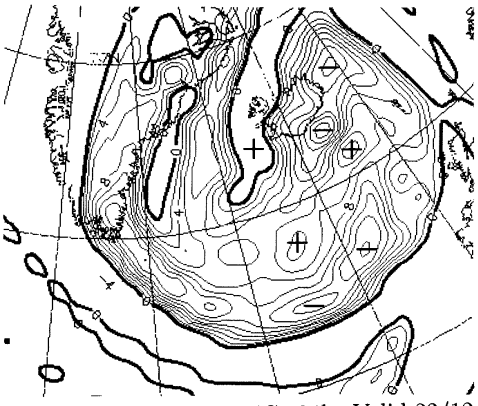

ECMWF 22.02.96 12UTC+24h. Valid 23/12

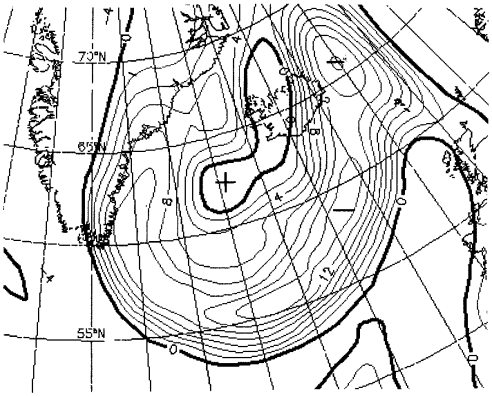

Arpège 22.02.96 12UTC+24h. Valid 23/12

ECMWF 22.02.96 12UTC+30h. Valid 23/18

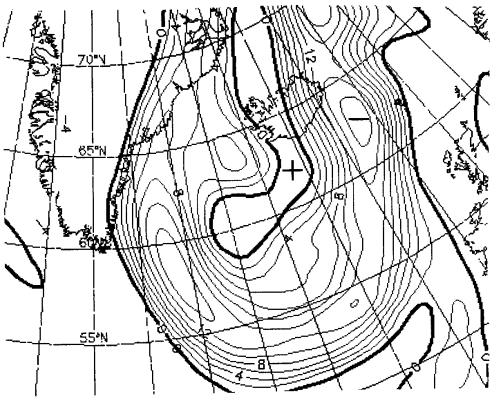

Arpège 22.02.96 12UTC+30h. Valid 23/18

ECMWF 22.02.96 12UTC+36h. Valid 24/00

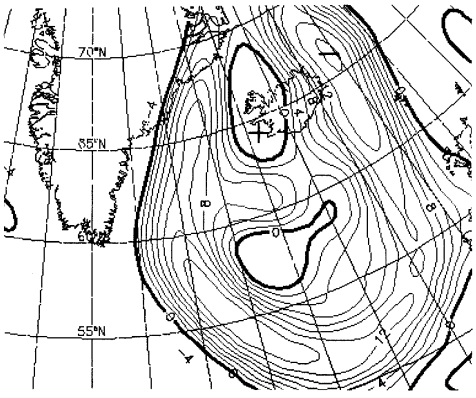

Arpège 22.02.96 12UTC+36h. Valid 24/00

Figure 5 (cont.)

A dipole in the voriticity field is a typical sign of gravity-wave breaking, and our simulated field of the ECMWF model is characterized by dipoles and tripoles. Such signatures are in particular found both south of Iceland, where the wind profile is indeed favourable for wave breaking, as well as in the lee of Greenland. The dipole signatures in the ECMWF model are particularly clear over the lee slope of Greenland (e.g. Figure 5, 22/1200 UTC) indicating active wave breaking. A possible explanation of the absence of such signatures in Arpège is that by a better represented orography, the flow in Arpège has entered further into the regime of flow splitting, giving a three-dimensional damping effect on the gravity waves.

The fine signatures in the ECMWF model could be related to other aspects of the parameterization of subgrid-scale orographic effects. In fact, the parameterization scheme of the effects of subgrid-scale orography in the ECMWF model is known to overestimate wave activity inflow at high values of Nh/U (Lott & Miller, 1997). This is presumably due to separate treatment of the parts of the flow that are deflected horizontally and vertically past the mountain (see discussion in Ólafsson & Bougeault, 1996). As explained above, the flow past Greenland has a value of Nh/U in the range 3–6 and is split to a great extent in our case.

The ECMWF model has also been known to overestimate long lee waves that break and lead to neutral layers in the mid-troposphere that are not observed (Lott, 1995). In our case, we find that the vorticity signatures leading to the filling of the trough are by far strongest in the middle troposphere and much weaker at lower or upper levels. This feature of the ECMWF model may, however, have been related to the old gravity-wave drag system or the envelope orography, which was replaced by a new scheme for subgrid-scale orography on 4 April 1995.

Another possible explanation of the vorticity pattern in the ECMWF model is the occurrence of long near-inertial waves that are created by the orography and oscillate in the horizontal plane. Such waves are produced in flow with low Rossby number and have been suggested to play an important role in the transition to breaking of vertically propagating waves (Trüb & Davis, 1995). In fact, such waves are known to be produced in the lee of Greenland in the ECMWF model.

6. Concluding remarks

From this case study, one can not, of course, draw any conclusions on systematic errors in any of the models, which are indeed both known to give very good results over the North Atlantic. The study suggests, on the other hand, that a correct representation of Greenland and Iceland in NWP models may be of great importance for accurate prediction of weather over the North Atlantic, even far downstream of the mountains. Orographically split flow may radically change the low-level vorticity and temperature fields, and through vertically propagating gravity waves, the orography may influence flow patterns in the upper troposphere and in the stratosphere. Thus, major mountain ranges such as Greenland, and even Iceland, may play an important role, for instance, in the development of precursors to the deepening of extratropical cyclones. Some of the questions that are still open on real orographic flow will hopefully be answered by the ongoing Greenland field experiments.

In general, it is not easy to analyse errors rapidly in the operational NWP models so that it may be of benefit for the real-time weather forecast. However, theoretically this could have been done with some success in the present case. Upon identifying, for instance, the responsible anomaly of low cyclonic vorticity at 24/0000 UTC, the anomaly is easily traced back to its location at 23/1200 UTC. At this point, Arpège gives a realistic surface pressure while the ECMWF model overestimates the surface pressure by a few hPa. A forecaster could therefore be quite confident in rejecting the vorticity anomaly in the ECMWF model and basing the forecast on the persisting trough as it appeared in Arpège.

This study suggests that charts showing the topography as it is represented in the different models are beneficial for the interpretation of the model output, not only in mountainous regions but also at a considerable distance downstream of major mountain ranges. For a skilful forecaster with solid knowledge of atmospheric flow around mountains, such charts would help identify and to evaluate the physical processes that occur in the numerical models, and consequently they would give guidance in interpreting and choosing between different model outputs. Numerical weather prediction centres should be urged to produce and publish such charts.

Acknowledgements

The author wishes to thank Francois Lott for discussions, Gérald Desroziers for producing Figure 1, Alain Joly for the access to real-time data at Météo-France during PRE-FASTEX in February and March 1996, and Gudmundur Hafsteinsson for helpful comments on the first draft of this paper.

References

Geleyn, J.-F., Bazile, E., Bougeault, P., Déqué, M., Ivanovici, V., Joly, A., Labbé, L., Pièdliévre, J.-P., Piriou, J.-M. & Royer, J.-F. (1994). Atmospheric parameterization schemes in Météo-France's Arpège NWP model. In *ECMWF Seminar Proceedings*, ECMWF, Reading, UK, 385–402.

Lott, F. (1995). Comparison between the orographic response of the ECMWF model and the PYREX 1990 data. *Q. J. R. Meteorol. Soc.*, 121: 1323–48

Lott, F. & Miller, M. J. (1997). A new subgrid-scale orographic drag parameterization: its formulation and testing. *Q. J. R. Meteorol. Soc.*, 121: 102–28

Ólafsson, H. (1996a). Atlas des écoulements hydrostatiques autour d'un relief idéalisé. *CNRM Technical Report 42*. Available form CNRM, F-31057, Toulouse, France.

Ólafsson, H. (1996b). Morphologie et traineée de quelques écoulement orographiques de complexité croissante. P*h.D. Thesis at Univ. Paul Sabatier*, Toulouse, France, 313 pp.

Ólafsson, H. & Bougeault, P. (1996). Nonlinear flow past an elliptic mountain ridge. *J. Atmos. Sci.*, 53: 2465–89.

Ólafsson, H. & Bougeault, P. (1997). The effect of rotation and surface friction on orographic drag. *J. Atmos. Sci.*, 53: 192–210.

Schär, C. & Durran, D. R. (1997). Vortex formation and vortex shedding in continuously stratified flows past isolated topography. *J. Atmos. Sci.*, 54: 534–55.

Schär, C. & Smith, R. (1993). Shallow-water flow past isolated topography. Part I: Vorticity production and wake formation. *J. Atmos. Sci.*, 50: 1373–1400.

Smith, R. (1979). The influence of the earth's rotation on mountain wave drag. *J. Atmos. Sci.*, 36: 177–80.

Smith, R. B. (1989). Hydrostatic airflow over mountains. In *Advances in Geophysics*. Vol. 31, Academic Press, 59–81.

Trüb, J. & Davis, H. C. (1995). Flow over a mesoscale ridge: pathways to regime transition. *Tellus*. 47A: 502–24.